Environmental Science and Pollution Research (2019) 26:31699–31716
https://doi.org/10.1007/s11356-019-06200-z

RESEARCH ARTICLE

A two decades study on ozone variability and trend over the main urban areas of the São Paulo state, Brazil

Daniel Schuch[1] · Edmilson Dias de Freitas[1] · Sergio Ibarra Espinosa[1] · Leila Droprinchinski Martins[2] · Vanessa Silveira Barreto Carvalho[3] · Bruna Ferreira Ramin[1] · Jayne Sousa Silva[1] · Jorge Alberto Martins[2] · Maria de Fatima Andrade[1]

Received: 27 March 2019 / Accepted: 9 August 2019 / Published online: 4 September 2019

Abstract

In this paper, we analyze the variability of the ozone concentration over São Paulo Macrometropolis, as well the factors, which determined the tendency observed in the last two decades. Time series of hourly ozone concentrations measured at 16 automated stations from an air quality network from 1996 to 2017 were analyzed. The temporal variability of ozone concentrations exhibits well-defined daily and seasonal patterns. Ozone presents a significant positive correlation between the number of cases (thresholds of 100–160 μg m^{-3}) and the fuel sales of gasohol and diesel. The ozone concentrations do not exhibit significant long-term trends, but some sites present positive trends that occurs in sites in the proximity of busy roads and negative trends that occurs in sites located in residential areas or next to trees. The effect of atmospheric process of transport and ozone formation was analyzed using a quantile regression model (QRM). This statistical model can deal with the nonlinearities that appear in the relationship of ozone and other variables and is applicable to time series with non-normal distribution. The resulting model explains 0.76% of the ozone concentration variability (with global coefficient of determination $R^1 = 0.76$) providing a better representation than an ordinary least square regression model (with coefficient of determination $R^2 = 0.52$); the effect of radiation and temperature are the most critical in determining the highest ozone quantiles.

Keywords Air quality · Quantile regression model · Seasonal trend

Introduction

Air pollution is recognized to be an important problem that is affecting public health and responsible for a variety of health effects (Künzli et al. 2000; Landrigan et al. 2018; Leiva et al. 2013; Levy et al. 2005; Monn 2001; Pope et al. 2002; van Zelm et al. 2008; Weschler 2006; WHO 2016).

Tropospheric ozone (O_3) is one of the air pollutants with major concern globally. Several studies have shown that the increase of the exposure to high ozone concentrations is followed by the increase of the daily mortality and f the number of heart diseases (Karthik et al. 2017). High concentrations of ozone are related to increasing of the daily mortality by 0.44% for each 10 ppb change in the hourly maximum ozone concentration (Anderson et al. 2004), affecting mainly children (Arjomandi et al. 2018; Di et al. 2017; Grivas et al. 2017), people with asthma or other lung diseases (Goodman et al. 2018), and also the part of the population leading to adverse health effects including the reducing of lung function, increased respiratory symptoms, and pulmonary inflammation (Hwang et al. 2015). Ozone also has affected negatively crops and trees, reducing productivity both directly through oxidative damage (which lead to reduction of the photosynthesis and consequently reducing the growth rate and carbon sequestration) and indirectly through its role as a greenhouse gas (Felzer et al. 2007; Ainsworth 2017).

Ozone is a secondary pollutant, which means that it is not directly released into the atmosphere, but formed by a chain of photochemical reactions that depend on the availability of

Responsible editor: Gerhard Lammel

✉ Daniel Schuch
schuch@usp.br

[1] Instituto de Astronomia, Geofísica e Ciências Atmosféricas (IAG), Universidade de São Paulo, São Paulo, Brazil

[2] Universidade Tecnológica Federal do Paraná, Londrina, Paraná, Brazil

[3] Universidade Federal de Itajubá, Itajubá, Minas Gerais, Brazil

incoming solar radiation and on the concentrations of many primary pollutants (directly released into the atmosphere) such as volatile organic compounds (VOC) and nitrogen oxides (NO_X). Once in the atmosphere, the ozone is directly affected by many physical processes of transport (turbulent mix, transport from upper levels of the atmosphere, advection by the mean wind and dry deposition). Changes in the vertical temperature gradient influence the stability and then the turbulent mixing in the atmospheric boundary layer (ABL) and, therefore, the ozone concentration near to the surface. Mesoscale systems like the mountain-valley, urban heat islands, sea breeze circulations (Freitas et al. 2007), and synoptic-scale winds, such as those found in frontal systems (Nair et al. 2004) can act on the transport of ozone and its precursors producing high ozone concentrations far away from the location of the primary pollutants sources. The presence of clouds contributes to modifying ozone production chain, reducing the available solar radiation, which drives the chemistry of the atmosphere by dissociating a number of molecules in fragments that are often highly reactive and also by heterogeneous reactions, which droplets and ozone precursors are removed by wet deposition.

The region of the São Paulo Macrometropolis is one the greatest urban conglomerates in the world that emerged through the process of conurbation between metropolitan areas inside the state of São Paulo with a total number of inhabitants of approximately 33 million people. The São Paulo Macrometropolis comprises the Metropolitan Area of São Paulo (MASP) and other urban areas, having 33 million inhabitants (IBGE, 2018), where high levels of ozone concentration become a critical health problem. Martins et al. (2017) shows extreme value analysis for pollutants for this region and found that the probabilities of occurring concentration above thresholds of ozone are more frequent on summers, while other analyzed pollutants are higher in winter.

Despite the emission control policies, high levels of ozone are still being observed (Pérez-Martínez et al. 2015; Carvalho et al. 2015) over São Paulo, which is a critical public health problem in MASP. Andrade et al. (2017) pointed a decreased in maximum ozone concentration in São Paulo between 1996 and 2006, besides an upward trend was observed after 2006. The analysis already conducted considered the average value of ozone concentrations at different air quality stations from the State Air Quality Network, not discriminating by different sites characteristics, e.g., urban, industrial, and near roads. Therefore, a deep analysis of all dataset available is necessary to investigate this possible trend, as well as to understand the factors that are influencing this ozone behavior. In this direction, this work seeks to analyze the variability of ozone concentrations measured in the region, in order to address these issues.

Methodology

Study region and dataset

The São Paulo Macrometropolis contains 174 cities covering an area of 53400 km^2 and is being one of the largest urban agglomerations of the southern hemisphere. With a high socioeconomic importance, this region concentrates high technology industries, diversified commerce, and the most productive agroindustry. It covers the Metropolitan Area of São Paulo (MASP), Baixada Santista (BS), Paraíba Valley (PV), Metropolitan Area of Sorocaba (MAS), and Metropolitan Area of Campinas (MAC), including also the Urban Agglomerations of Jundiaí and Piracicaba. Figure 1 shows a map of these regions, and the location of the sites of CETESB network used in this analysis depicted as colored circles.

The MASP is located between two mountain chains ("Serra da Mantiqueira" and "Serra do Mar") with approximately 750 m of altitude, 60 km from the seashore, and being the wind regime in the region strongly influenced by mesoscale phenomena such as sea breeze, urban heat island, and mountain-valley circulations (Freitas et al. 2007).

Hourly O_3, NO, NO_2, and CO concentrations measured at 16 automatic air quality monitoring stations from 1996 to 2017, provided by the São Paulo State Environmental Agency network (CETESB 2018), are used in this study. The sites are related in Table 1, along with the lat–long coordinates, the metropolitan region that it is part of, the first year of data available to each site, and the classification of the station taking into account the sources of pollutants that influences the concentrations measured and the exposure of the population, using the criteria from the United States Environmental Protection Agency (EPA 1996) and the World Health Organization (WHO 2000).

I industrial, *R* residential, *C* urban central, *V* vehicular

The industrial stations (I) are on areas where industrial sources have a major influence on the concentrations observed; (R) states for stations located in residential and suburban areas; (C) represents commercial stations in central urban areas, areas of commerce, with great movement of pedestrians and vehicles; vehicular stations (V) are located near a traffic lane. Some stations fall into more than one class.

Meteorological data from a weather station of the Institute of Astronomy, Geophysics and Atmospheric Sciences from the University of São Paulo (IAG-USP) were used to obtain climatological averages of rainfall, temperature and global solar radiation using data from the period of 1933 to 2017 (IAG 2018).

Model description

A linear regression model (LRM), also known as ordinary least squares, is a linear approach to modeling the relationship between a dependent variable and one or more independent variables. The model assumes the homoscedasticity (different values

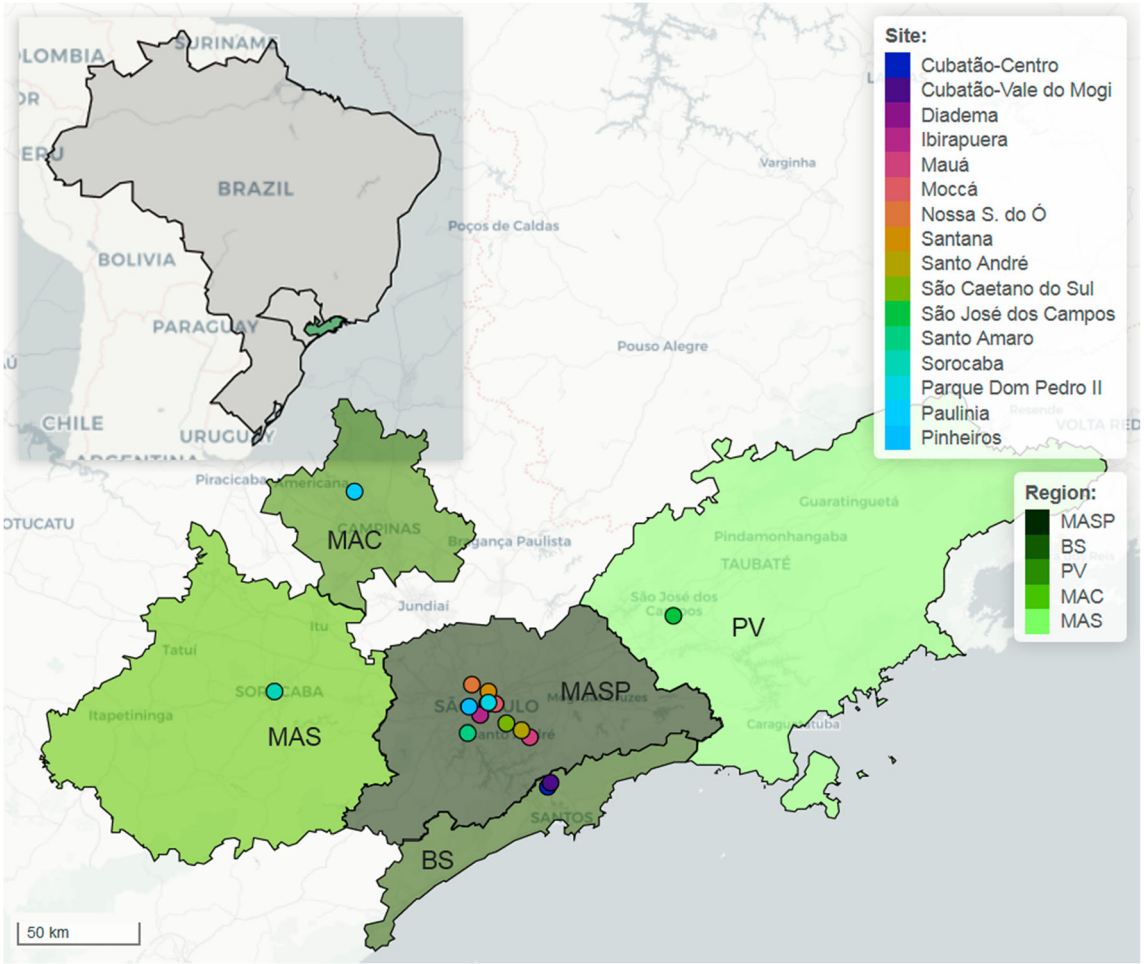

Fig. 1 Location of the air quality measurement sites and main urban regions of the São Paulo Macrometropolis

of the independent variables produces errors with constant variance, regardless of the values of the independent variables) that is invalid for the most practical cases (Baur et al. 2004).

Baur et al. (2004) propose a similar approach, which is called quantile regression model (QRM). Besides the measure of the central tendency, the method considers the full distribution of the dependent variable when estimating the potential differential effect on various quantiles. The QRM does not make assumptions about the data distribution allowing the covariates to have different impacts on data distribution considering different points (heteroscedasticity). In this way, QRM considers the nonlinearities existent between variables.

Using O_3 concentration as dependent variable and the concentrations of CO, NO, NO_2, wind speed (U), global radiation (Rad), and the temperature (T) as independent variables, LRM Eq. (1) and QRM Eq. (2) can be obtained as below (Reimann et al. 2008):

$$O_3 = \beta_0 + CO\beta_1 + NO\beta_2 + NO_2\beta_3 + U\beta_4 + Rad\beta_5 + T\beta_6 + \varepsilon \quad (1)$$

$$O_3 = \beta_0^{(p)} + CO\beta_1^{(p)} + NO\beta_2^{(p)} + NO_2\beta_3^{(p)} + U\beta_4^{(p)} + Rad\beta_5^{(p)} + T\beta_6^{(p)} + \varepsilon^{(p)} \quad (2)$$

where p denotes the pth quantile with $0 < p < 1$, β_0 is the constant of intercept, β_1 to β_6 are the slopes (gradients) of the independent variables, which are determined using each time of the entire data, and ε is the error.

The trends in the sections 3.4 and 3.5 were calculated using the robust estimate of slope for this nonparametric fitted line, and it was described by Henry Theil in 1950 (Theil 1992). An estimate of the intercept is also available (Conover 1980). Together these define an estimate of a complete linear equation on the form of Eq. (2), but this estimate is made by comparing each data pair in a pairwise fashion with the advantage of being independent on the data distribution (Helsel and Hirsch 2002).

Results and discussion

Air quality variability

The establishment of air quality standards must be based on scientific knowledge in order to provide a foundation for protecting people health from exposition of high ozone

Table 1 Description of the automatic air quality monitoring stations

Site	Latitude	Longitude	Region	Start year	Class
Cubatão-Centro	– 23.8516	– 46.3909	BS	1996	I/R/C
Cubatão-Vale do Mogi	– 23.8376	– 46.3805	BS	2005	I
Diadema	– 23.5499	– 46.6341	MASP	1999	I/R
Ibirapuera	– 23.5914	– 46.6602	MASP	1996	R
Mauá	– 23.6678	– 46.4635	MASP	2004	I/R
Moccá	– 23.5497	– 46.5984	MASP	1996	C/R/I
Nossa S. do Ó	– 23.4796	– 46.6916	MASP	1999	R
Santana	– 23.5055	– 46.6285	MASP	2000	C/R
Santo André-Capuava	– 23.6429	– 46.4925	MASP	2000	R/V
São Caetano do Sul	– 23.6176	– 46.5563	MASP	1996	R/I
São José dos Campos-Jd. Satélite	– 23.2244	– 45.8899	PV	2000	C/R
Santo Amaro	– 23.6545	– 46.7095	MASP	2002	R
Sorocaba	– 23.5026	– 47.4776	MAS	1996	R/I
Parque Dom Pedro II	– 23.5448	– 46.6276	MASP	1999	R/V
Paulinia	– 22.7714	– 47.1562	MAC	2000	I
Pinheiros	– 23.5612	– 46.7016	MASP	1996	R

concentration. The Air Quality Guidelines for Europe (WHO 2000) set the limit values for ozone exposure levels to 120 μg m^{-3} (using 8-h moving averages). However, studies have detected that health effects occurring at concentrations below this limit (Karthik et al. 2017). In 2005, WHO Air Quality Guidelines (AQG) has reduced the limit from 120 to 100 μg m^{-3} on a daily maximum 8-h moving mean (Krzyzanowski and Cohen 2008). In Brazil, the limits to atmospheric pollutants, the National Air Quality Standards (NAQS), are determined by the National Council of Environment (CONAMA), and the limit for ozone concentrations was changed in 2018 from 160 μg m^{-3} for hourly mean (CONAMA, 1990) to 140 μg m^{-3} for 8-h mean (CONAMA, 2018). For the state of São Paulo (SP), since 2013, the limit is determined by São Paulo State Government, and currently, it is equal to 140 μg m^{-3} for 8-h moving average and there is a plan in the future to change it to 130 μg m^{-3}, 120 μg m^{-3}, and then to 100 μg m^{-3} as final guidelines, besides there is no deadline for these changes to happen (ALESP 2013).

Figure 2 shows the number of days per number of stations, which recorded concentrations that exceeded different reference values over São Paulo Macrometropolis. The full (red) line was made by summing the number of days a station exceeds 160 μg m^{-3} for hourly mean values divided by the available number of stations for each year, while the dashed lines were made with the limits of 140, 120, and 100 μg m^{-3}, respectively, using 8-h moving averages (mean values were calculated for each 8-h interval, if at least 6 h of data are available).

Figure 3 shows the number of exceedances by station using different limits (hourly 160 μg m^{-3}, 8-h mean average of 140, 120, and 100 μg m^{-3}). The blue bar shows the normalizing

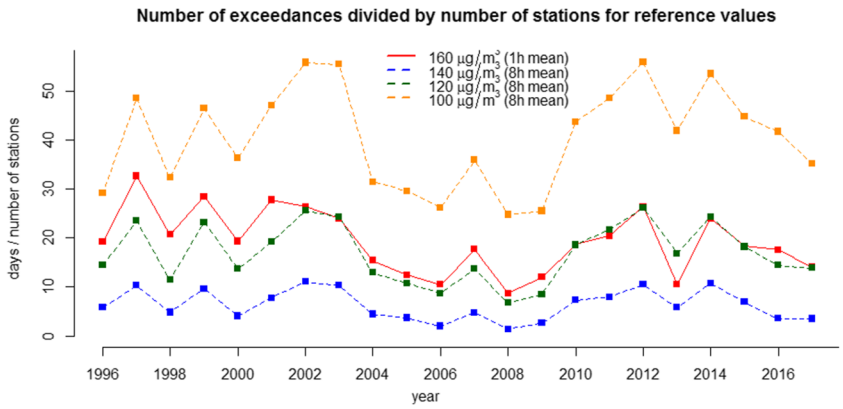

Fig. 2 Number of days weighted by number of stations that exceed reference values over the years

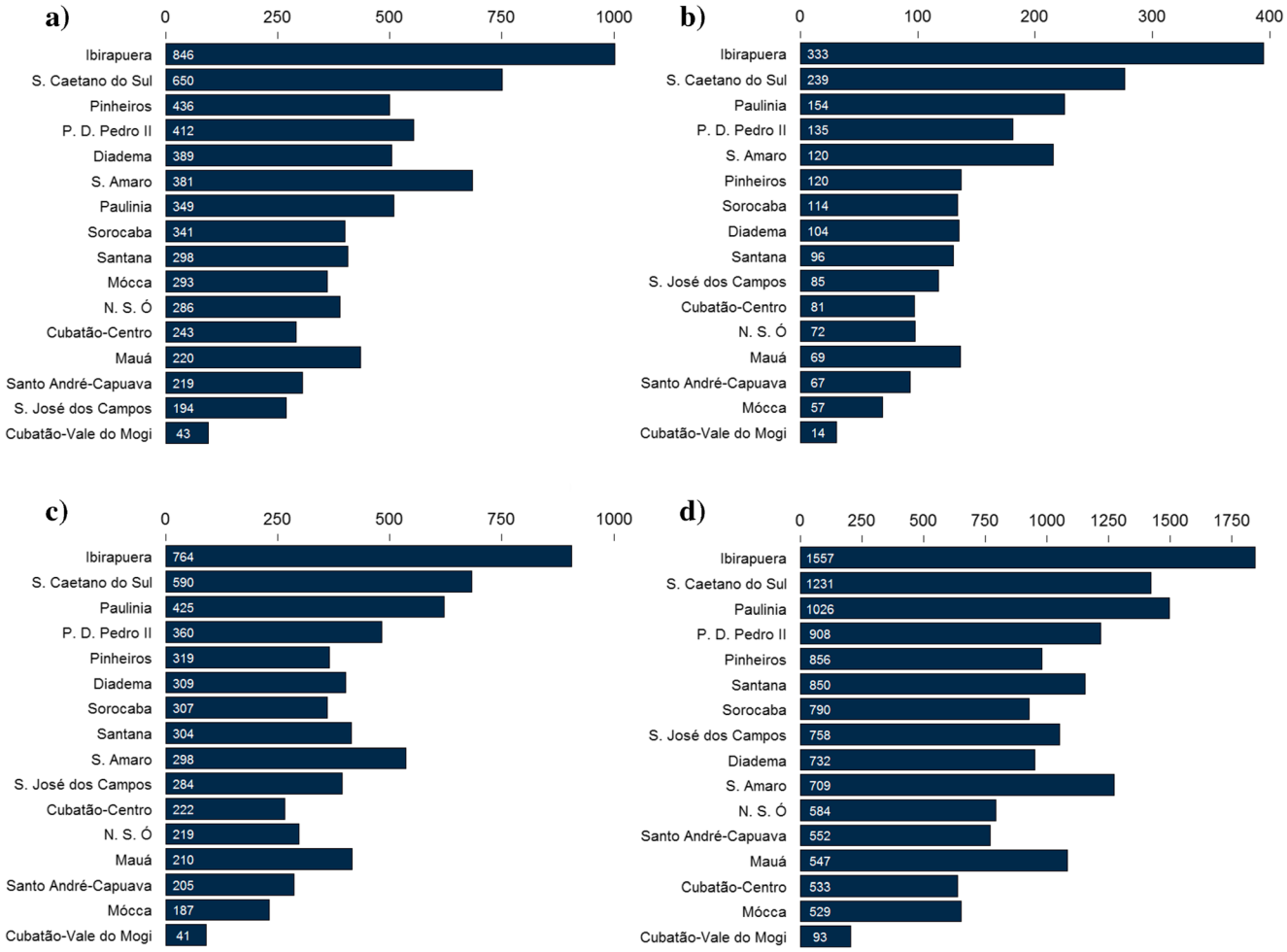

Fig. 3 Counting of the number of days with different ozone limits exceedances: **a** hourly 160 μg m^{-3}, **b** 8-h mean average of 140 μg m^{-3}, C) 8-h mean average of 120 μg m^{-3}, and **d** 8-h mean average of 100 μg m^{-3}

number of occurrences calculated by Eq. (3):

$$\overline{O}_i = O_i.\left(\frac{1}{1-f}\right) \tag{3}$$

where O_i is the number of occurrences (showed in white in Fig. 3) for that given limit i, f is the fraction of missing or unavailable ozone concentration data, and $\overline{O}_i$ is the normalizing number of occurrences.

The highest number of days with occurrences of standard exceedances are seen when using the hourly mean value against the lower limit value. The use of moving averages on ozone concentration tends to smooth the maximum peaks. For this study, we choose the hourly limit of 160 μg m^{-3}, because it represents better the observed variable and the time scales involved. Today, CESTESB states that the current reference value of 140 μg m^{-3} shows that the ozone problem is smaller, but in fact, although there is a reduction, there are still very high numbers of standard exceedances when comparing with value of 120 or 100 μg m^{-3} as a reference.

The ozone concentration in a highly urbanized environment like the São Paulo Macrometropolis depends mainly on three important factors with a very distinct nature: the availability of reactants (which determine the formation/destruction of ozone by photochemical/chemical reactions), the availability of energy (solar incidence), and the atmospheric transport. The ozone production is a non-linear photochemical process influenced by the emissions of their precursors, besides the large range reactivity of VOC (Carter, 1994; Jacobson 2005). In addition, the atmospheric variables have a wide variety of time-scales as follows: the atmospheric temperature and stability at the surface level (inside the planetary boundary layer) has a time-scale of 1 h or less (Stull 1988), while the mesoscale phenomena like urban-heat-island, mountain-valleys, and sea-breeze circulations exhibit a daily pattern (Bluestein 1992), and synoptic-scale responsible for severe weather systems, such as heat waves and cold front passages, causing precipitation and nebulosity and having a scale greater than a day (Holton 2004). Even the influence of intercontinental oscillations, like the El-Niño or the Pacific decadal oscillation (PDO), could affect the local temperature, humidity, and

wind at the time-scale of several years (Capotondi et al. 2015; Mantua et al. 1997). In the next sections, the variability of ozone at different scales is analyzed.

Daily variability

Figure 4 shows the variability of hourly concentration of O_3, NO, NO_2, and CO for 1996–2017. NO_2 is the only known molecule to photodissociate in the presence of the radiation with the wavelength available at troposphere releasing an oxygen atom, which combine with oxygen molecule to produce ozone. NO can consume this ozone in an unpolluted atmosphere. In general, the following pattern is observed along all CETESB stations: high concentration peaks of ozone in the afternoon are preceded by lower concentrations of NO in the morning. This is a classical behavior of ozone and their precursors observed in urban areas, showing the chemical relation among these species (Fig. 4).

Figure 5 shows the daily patterns of radiation (gray bars), temperature (red line) at Paulinia station, and traffic activity (black line) calculated from traffic counts of toll stations located in São Paulo city, for summers and winters of 2012, 2013, and 2014. The gray lines correspond to passenger cars (PC), light commercial vehicles (LCV), motorcycle (MC), and heavy-duty vehicles (HGV).

The combustion from engines is a direct source of nitric oxide (NO), nitrogen dioxide (NO_2), and CO, while the VOC can be emitted by the process of exhaust (through the exhaust pipe), from liquid (carter and evaporative) to vapor (fuel transfer operations). These anthropogenic emissions are directly affected by the activity of the traffic in each metropolitan region as well as by the flow of vehicles between different metropolitan regions and the fleet characteristics such as the type of fuel and years of use.

The daily patterns in Fig. 5 are typical profiles that can be observed along all stations for temperature and radiation. An interesting information that can be obtained from Fig. 5 is that the classical description of the traffic activity that should be a Gaussian distribution with two peaks of traffic flow at morning and night hours is not observed (with exception of the motorcycles case). Instead, the flow seems to be distributed from 6:00 until 18:00 local standard time (LST) in a different pattern. The traffic behavior changed in recent years and can be a factor to be considered in the ozone pattern.

The ozone daily patterns are typical with peak of ozone around 14:00–15:00 LST. As well established in the literature, the daily ozone concentration is controlled primarily by the

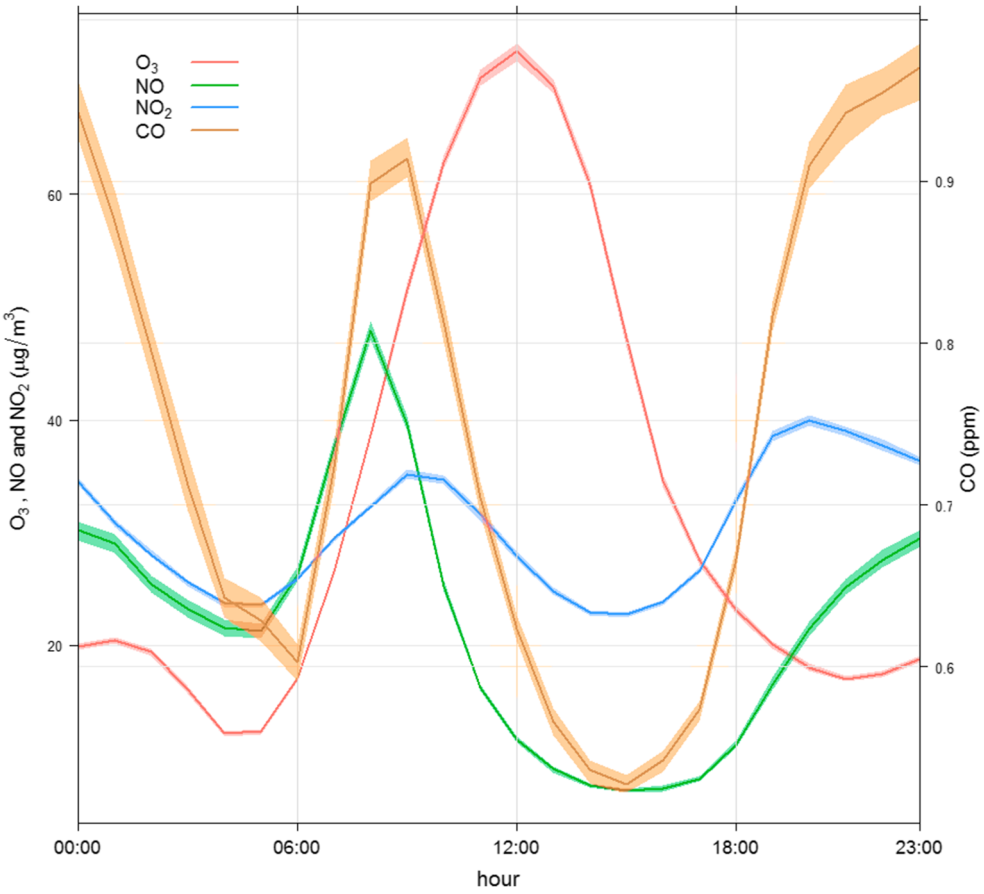

Fig. 4 Hourly mean concentration of ozone, nitrogen oxides, and carbon monoxide

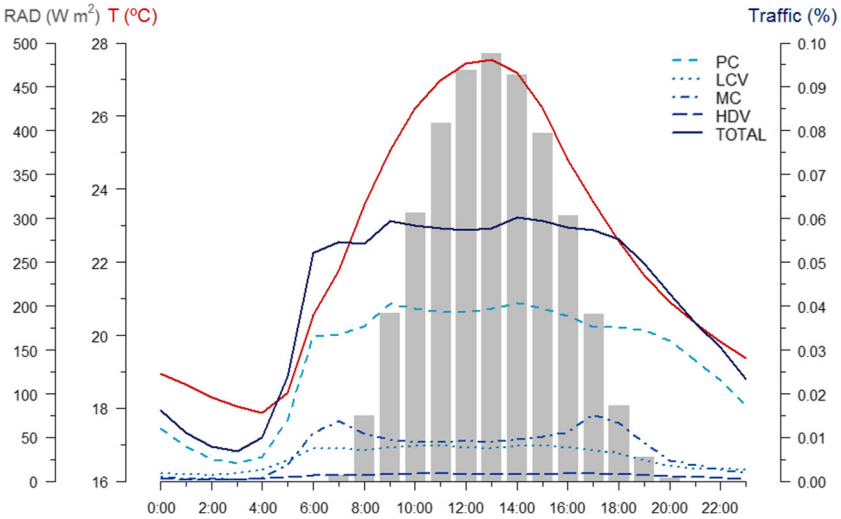

Fig. 5 Daily patterns of radiation, temperature, and traffic activity by passenger cars (PC), light commercial vehicles (LCV), motorcycle (MC), heavy-duty vehicles (HDV), and the total.

weather patterns of radiation and by the precursors. The precursors of ozone are primary pollutants emitted by different processes such as combustion (anthropogenic and natural) and biogenic (from vegetation) from many sources, but in a highly urbanized environment such as MASP, the majority of these pollutants come mainly from the vehicular sources (Andrade et al. 2012; CETESB 2014; Gaffney and Marley 2009; Nogueira et al. 2015; Ibarra-Espinosa et al. 2018). In urban areas, where the VOC-limited photochemical regimes have usually encountered, the photochemical reactions involving non-methane volatile compounds (NMVOC) are considered as one of the major precursors of ozone (Fujita et al. 2003; Qin et al. 2004; Silva Júnior et al. 2009), which is also the case of São Paulo Macrometropolis (Andrade et al. 2017; Martins et al. 2008; Orlando et al. 2010).

The role of VOC on ozone formation is the focus of many studies dedicated to the São Paulo Megacity (MSP). Brito et al. (2015) present the impact of ethanol usage on vehicular emission ratios of VOC. Nogueira et al. (2014) analyzes the impact of the use of ethanol or gasohol by flex vehicles using 2 years of experimental data with measures of ozone, NO_X, and VOC. Nogueira et al. (2015) analyzed data from experimental campaigns on road tunnels, and Dominutti et al. (2016) studied the biofuel effect on VOC burden and composition and showed that the seasonal variation of the potential for ozone formation from VOC is higher on winter and lower in spring. Alvim et al. (2018) determined that the aldehydes are the main VOC ozone precursors and their importance in terms of reactivity and availability in the MASP.

Seasonal variability

The climate in the São Paulo Macrometropolis can be summarized between the warmer and wet summer and dry winter. The hourly mean concentration of ozone (as the NO and NO_2) exhibits a comparable seasonal behavior as shown in Fig. 6.

Figure 8 shows the mean concentration (full lines, first axis at left) of ozone (red), NO (green) and NO_2 (blue) for all stations, their extreme values (dotted lines, second axis at left), and the total number (gray bars, right axis) of days that every station registers an occurrence of ozone concentration greater than 160 μg m^{-3} by each month. The mean and extreme values for ozone concentration are higher in October and lower from April to June. A local maximum and extreme concentrations were present on February and March. The NO and NO_2 have an opposite behavior compared with ozone, being high values of ozone observed when low values of NO_X are present. The ozone concentration seems to have a very different seasonal behavior from the relative ozone formation potential. The main reason for it is that this reaction depends strongly on meteorological factors.

Figure 9 shows the climatological averages of global solar radiation (black line), hours of sunlight (gray dashed lines), rainfall (blue bars), and temperature (red line) for the IAG-USP meteorological station using data from the period of 1933 to 2017.

The months from December to February are the months that concentrate most of the annual rainfall while the months of June to August are the driest months. The spring and summer are the seasons with the higher incidence of solar radiation and highest temperatures, which are factors that contribute to the ozone formation. The annual peak of temperature shown in Fig. 9 occurs in November while February has the highest radiation month. The presence of convective instability in the warmer months causes precipitation and cloud formation which reduces incident solar radiation and provides vertical transport of heat from the heated surface to higher levels of the atmosphere. October is the most critical month with relation to the number of cases and mean and maximum

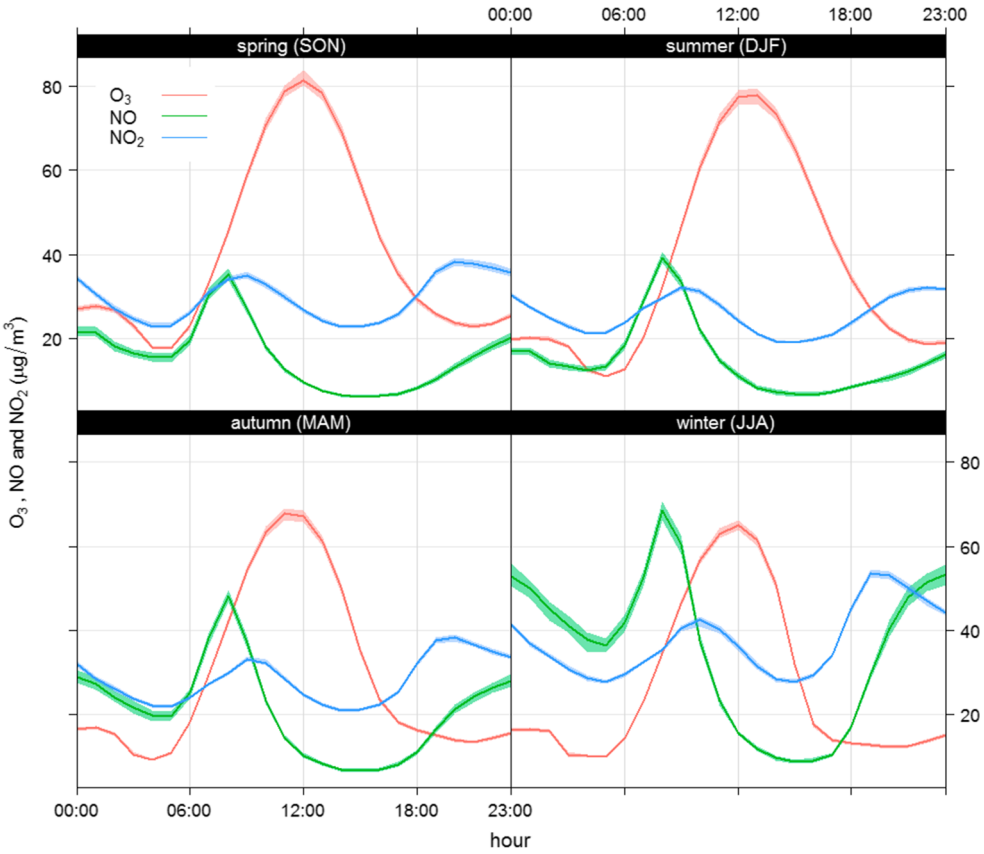

Fig. 6 Hourly mean concentration of ozone and nitrogen oxides for different seasons

ozone concentration; the photochemical process of ozone production needs radiation with $\lambda < 243$ nm. This radiation is not available at certain weather conditions such as rainy or overcast days. The total hours of sunlight does not provide this precise information but can be used as an indicator of the amount of sunny days with a few clouds, which is a good condition for ozone formation.

The annual cycle of ozone is strongly influenced positively (increasing the concentration) by variables such as solar incident radiation and air temperature and negatively (decreasing the concentration) by precipitation, which can affect concentrations indirectly, through an efficient process of wet removal of ozone precursors and directly by heterogeneous reactions on water droplets, that reduce the incident radiation (because the associated nebulosity) and temperature (through cold air advection), which reduces the ozone production. The spring and summer season concentrate the majority of ozone concentrations that exceed 160 μg m^{-3} with 41% and 34% when winter and autumn had 16% and 9% of the cases, respectively.

Long-term variability

Figure 10 shows the annual maximum concentration of ozone (full lines), the trend (dotted line) split by season (with different colors), and the 95% confidence interval of each regression, showed as the shaded area around the dotted lines. The trends were calculated by a linear model using the time as the independent variable. The ozone maximum trend (Fig. 10a) shows a decreasing average of 2.41 μg m^{-3} by year (with the linear trend of − 2.41 for spring, − 2.48 for summer, − 1.7 for autumn, and − 4.98 μg m^{-3} $year^{-1}$ for winter). Figure 10b shows the annual mean concentration of ozone and the trend by season. The spring and summer show a significant upward trend of 0.16 μg m^{-3} $year^{-1}$ (with the linear trend of 0.16 for spring, 0.20 for summer, 0.07 for autumn, and − 0.14 μg m^{-3} $year^{-1}$ for winter).

The ozone concentrations have a nonlinear behavior, and a simple linear model do not describes the variability for this variable. The exception is the decrease of ozone maximum at winter. For this reason (and from previous discussions), we apply the quantile regression model to our data.

The QRM and LRM regression coefficients are depicted in Fig. 11, 0using ozone as the independent variable and CO, NO, NO_2, wind speed, global radiation, and temperature as dependent variables at Ibirapuera station by the Barrodale and Roberts "BR" algorithm for computing this fit (Koenker and D'Orey 1987). Figure 11 shows the quantile regression outputs represented by dashed–dotted line with their 95% confident intervals alongside with the ordinary least square regression output indicated by solid line along with its 95% confident interval. In quantile regression, we chose the values of 0.1, 0.2, 0.3, 0.4, 0.5, 0.6, 0.7, 0.8, 0.9, and 0.95 for quantiles

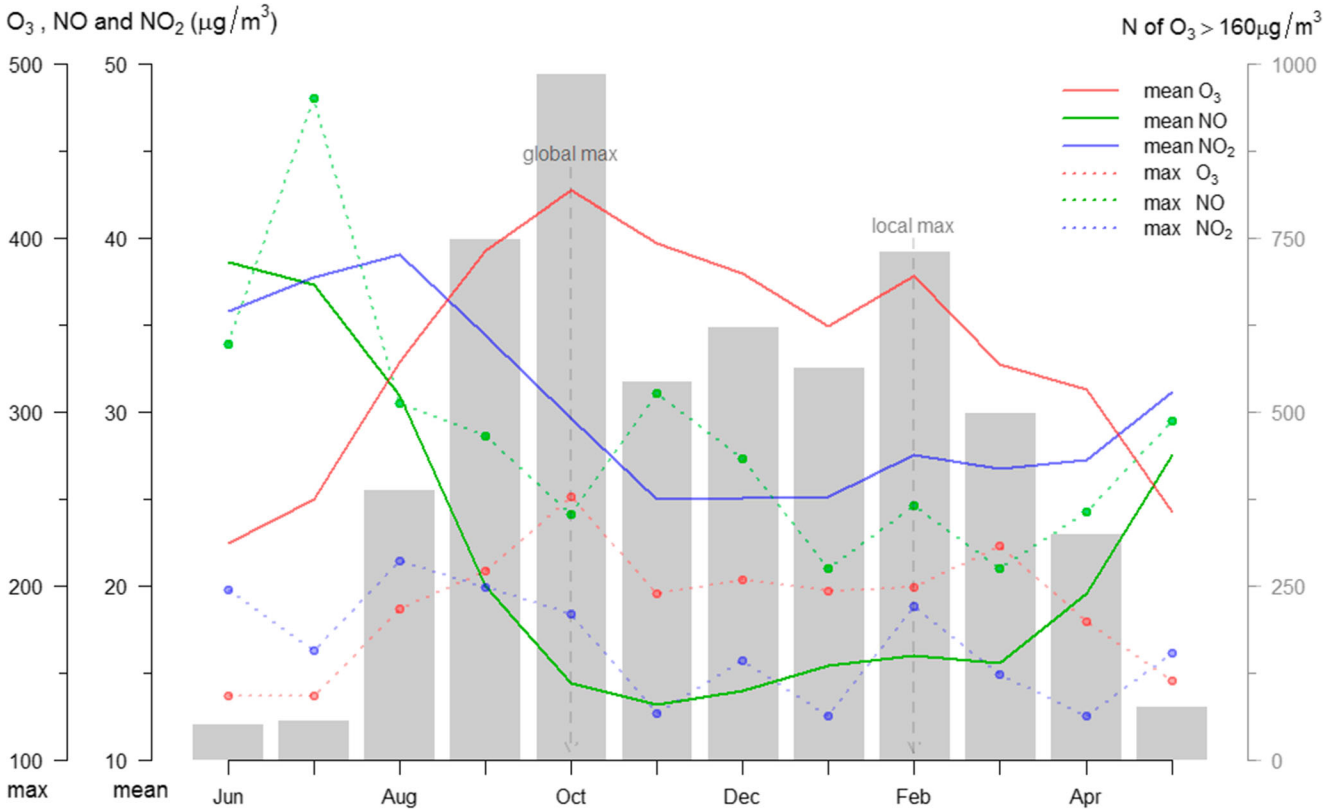

Fig. 7 Monthly mean concentration of ozone and nitrogen oxides

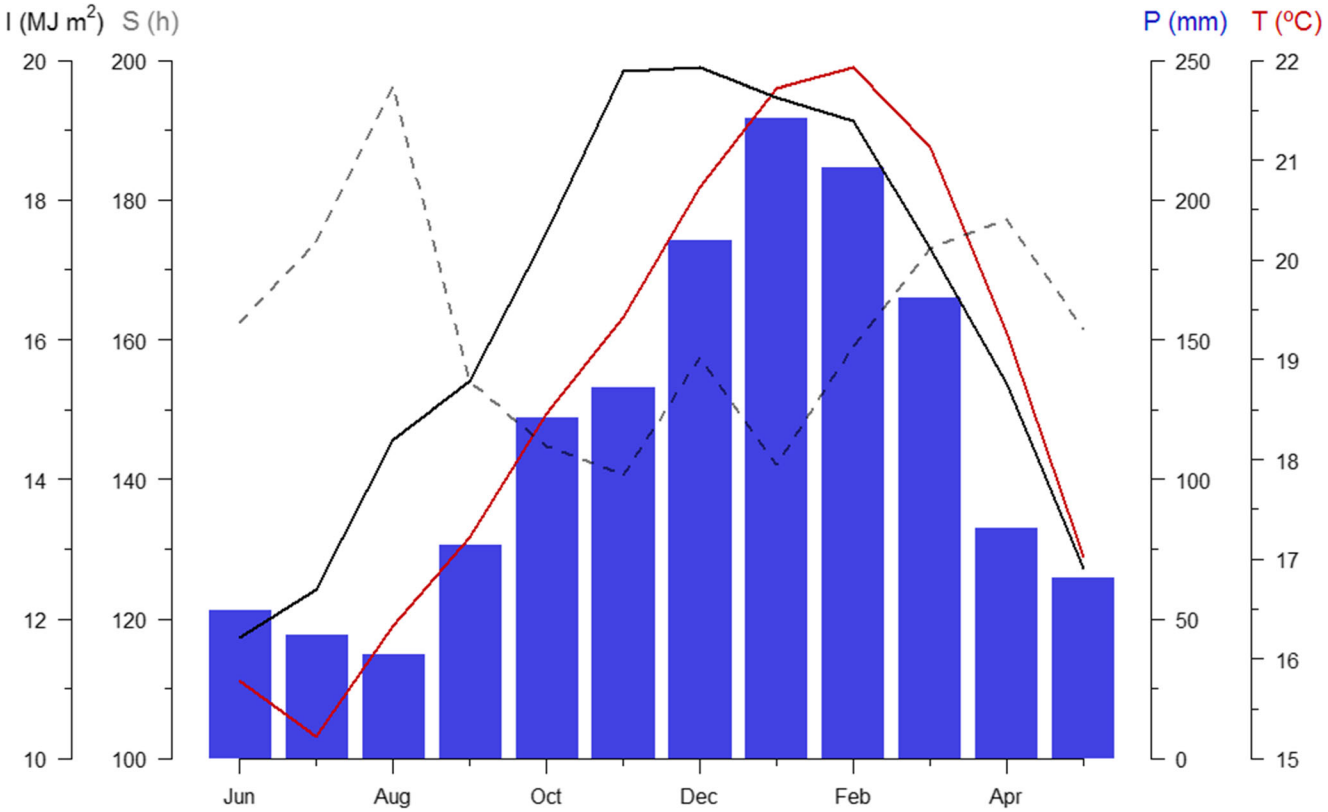

Fig. 8 Climatology of the monthly averages of the incoming solar radiation, hours of sunlight, precipitation, and temperature

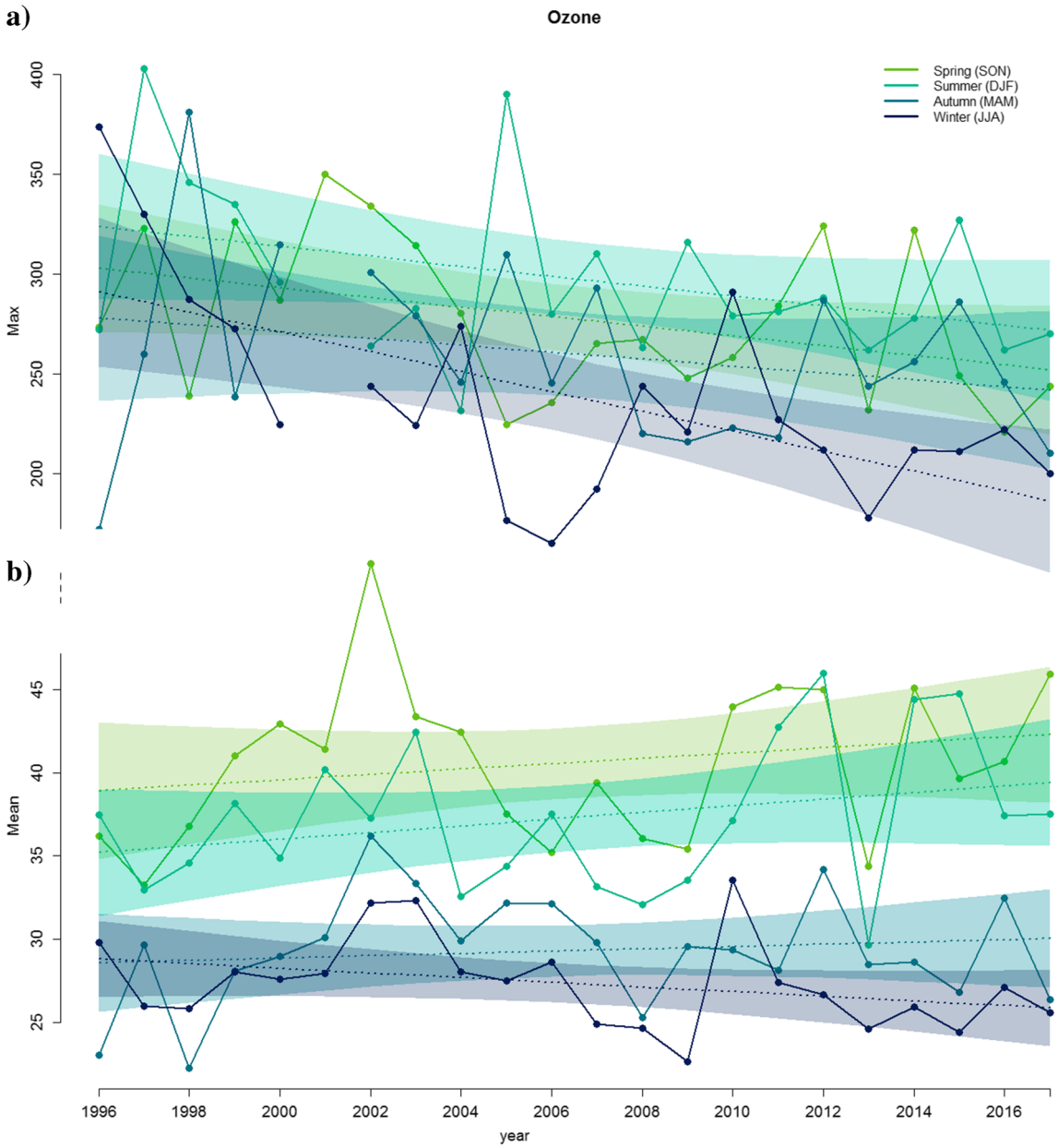

Fig. 9 Annual maximum (**a**) and mean (**b**) concentration for ozone by season

(*x*-axis), whereas in the LRM, only one regression coefficient represents the entire distribution of the independent variable.

The effect of CO on ozone (Fig.11a) is significant for quantiles between 0.5 and 0.8, which shows that CO have negative association with ground-level ozone (negative values in the Fig. 11a), an increase of ozone levels can be associated to decrease of CO concentrations at certain range of ozone concentration, which explains the significant negative correlation.

The effect of NO (Fig. 11b) on ozone concentration is significant for almost all quantiles but with a different signal depending on the ozone concentration. The change on signal can be explained for changes on the photochemical process when there is enough UV radiation the process showed the formation of O_3 based on the NO_X concentrations and when it is the sunset the NO_X emitted by the traffic is involved in the reaction of consuming O_3. On the other hand, the effect of NO_2 (Fig. 11c) is negative and significant for all interval, being maximum at quantile 0.7.

The wind speed (Fig. 11d) effect, as the effect of the global radiation and temperature (Fig. 11e, f), are significant for all quantiles. The wind speed in the particular case of the Ibirapuera is related to the transport of ozone (as its precursors) from the vicinity and global radiation and temperature are directly related to photochemical process of ozone

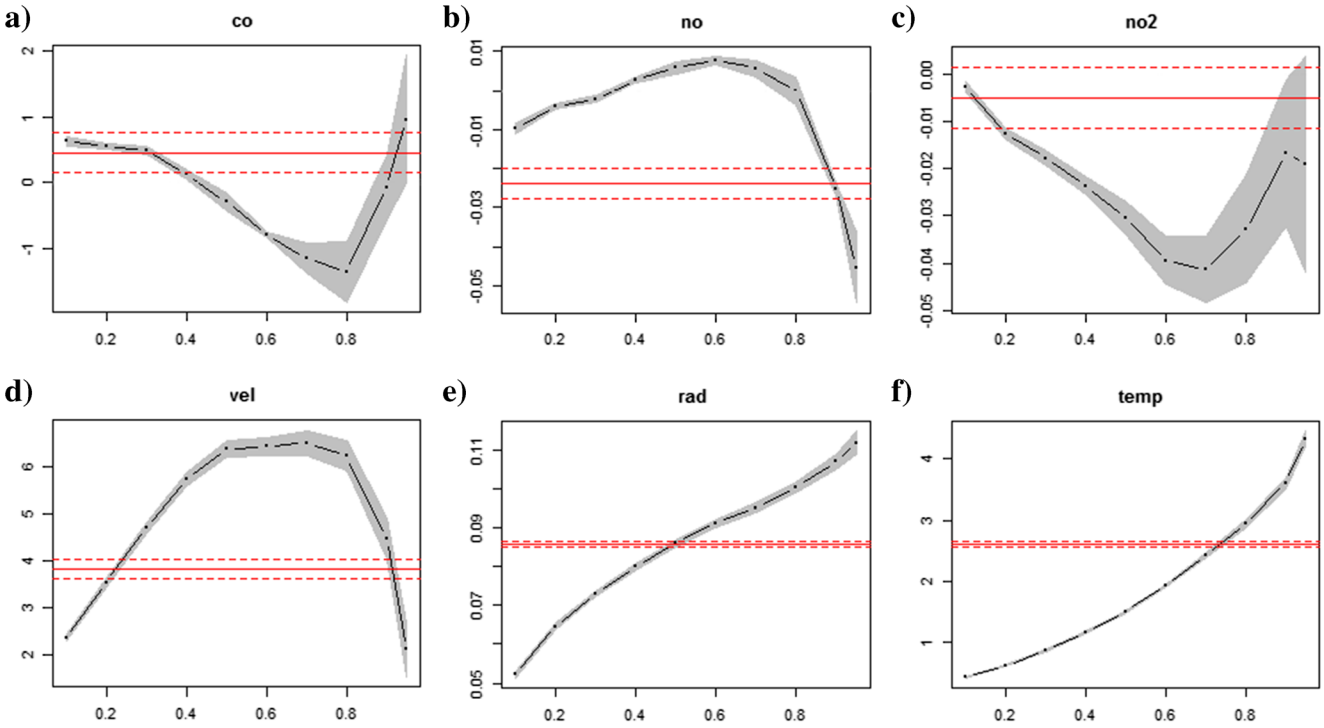

Fig. 10 Outputs from the QRM showing the effect of CO (**a**), NO (**b**), NO_2 (**c**), wind speed (**d**), incident radiation (**e**), and temperature (**f**) on hourly mean ozone concentrations

production during the day and its destruction at night, which is being more important at higher quantiles.

The coefficient of determination R^2 is a portion of the variance of the dependent variable that is predicted by the independent variable, and it is used as a measure of how well a model explains and predicts the variable of interest. In QRM, the equivalent measure of the coefficient of determination (R^2) is represented by the local coefficient of determination $R^1(\tau)$ and its values, such as R^2, lies between 0 and 1 (Koenker and Machado 1999). The R^2 measures a global goodness of fit over the entire conditional distribution, whereas $R^1(\tau)$ measures the local performance of the model for a given quantile (τ). $R^1(\tau)$ values for quantiles from 0.1 to 0.95 are shown in Fig. 12, which are comparable to R^2 (gray-dotted line).

The global coefficient of determination (denoted by R^1) was calculated for the QRM as suggested by Baur et al. (2004). The first step in the estimation of R^1 is to determine quantile regression coefficients. The test dataset (ozone concentration of the Ibirapuera station from 1996 to 2017) was divided into 10 equal subsets according to the quantile values. Ozone was predicted using QRM and combined into one dataset order from 0.1 to 0.95 quantiles. Finally, predicted (estimated by QRM) and observed ozone (measured at Ibirapuera station from 1996 to 2017) were compared.

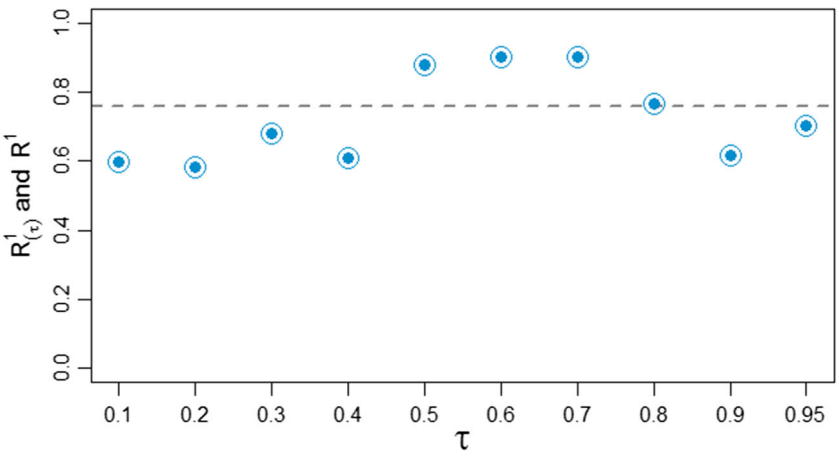

Fig. 11 Local and global coefficient of determination for the QRM at Ibirapuera

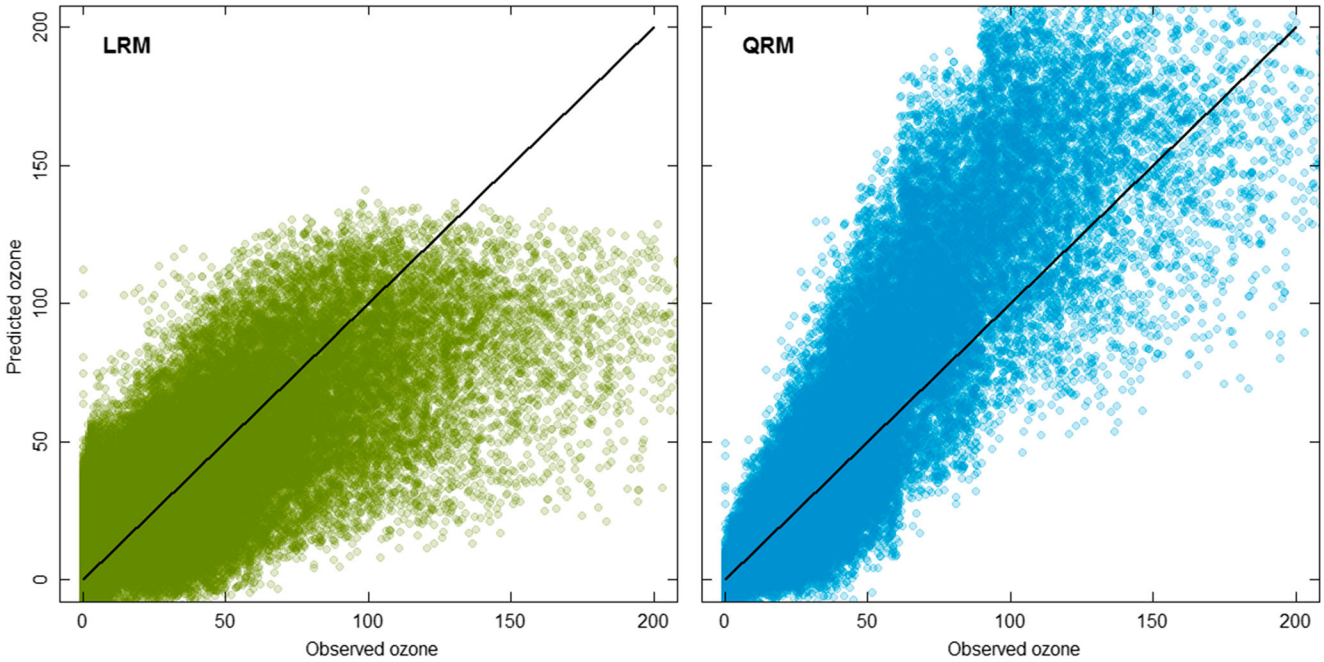

Fig. 12 Comparisons of observed ozone and regression results: linear regression model (**a**) and with a quantile regression model (**b**).

Figure 13 shows the predicted ozone against the observed at Ibirapuera monitoring station from 1996 to 2017. The scatterplot of the predicted ozone by the LRM (Fig. 13a) shows that the predicted values are underestimated not exceeding 140 μg m^{-3}. By other hand, the ozone predicted by the QRM (Fig. 13b) is overestimated. The QRM explains more of the ozone variation showing an R^1 value of 0.76 in comparison with LRM, which has R^2 value of 0.52. This indicates that QRM explains the ozone variation (76%) significantly better than LRM (52%).

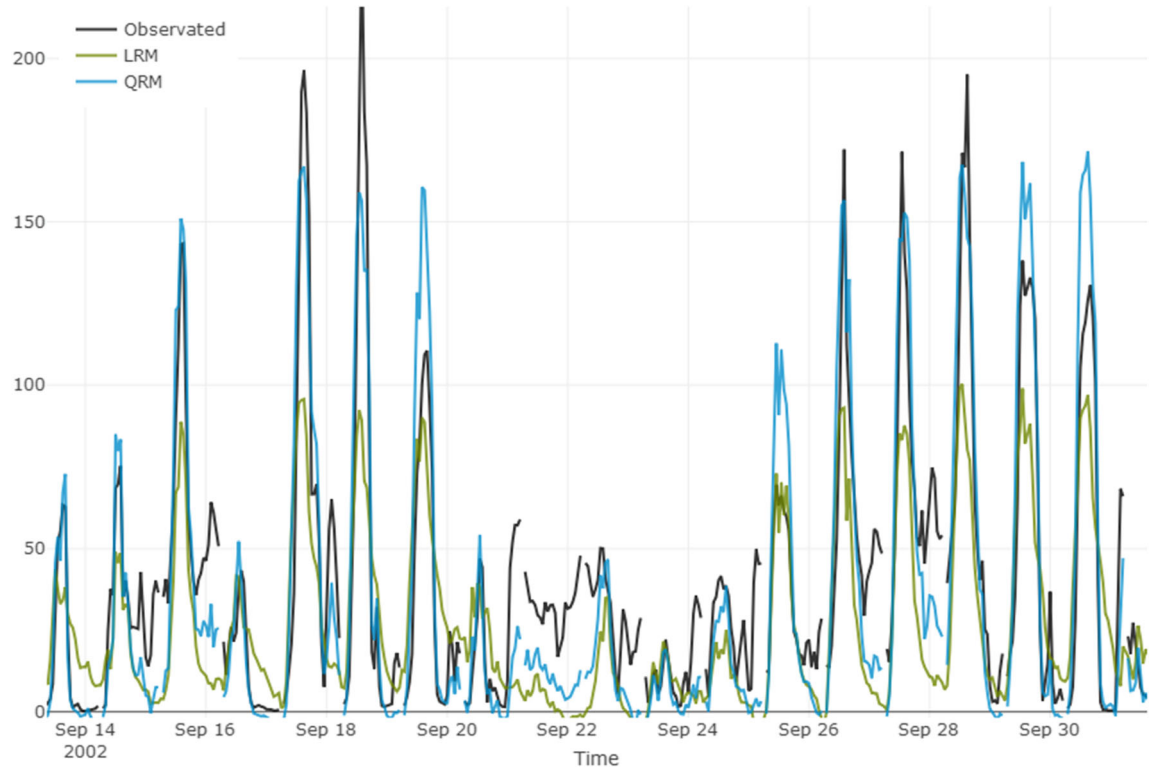

Fig. 13 Time series of observed ozone (black), linear regression model (Landrigan et al. 2018), and quantile regression model (Bluestein 1992) for September of 2002.

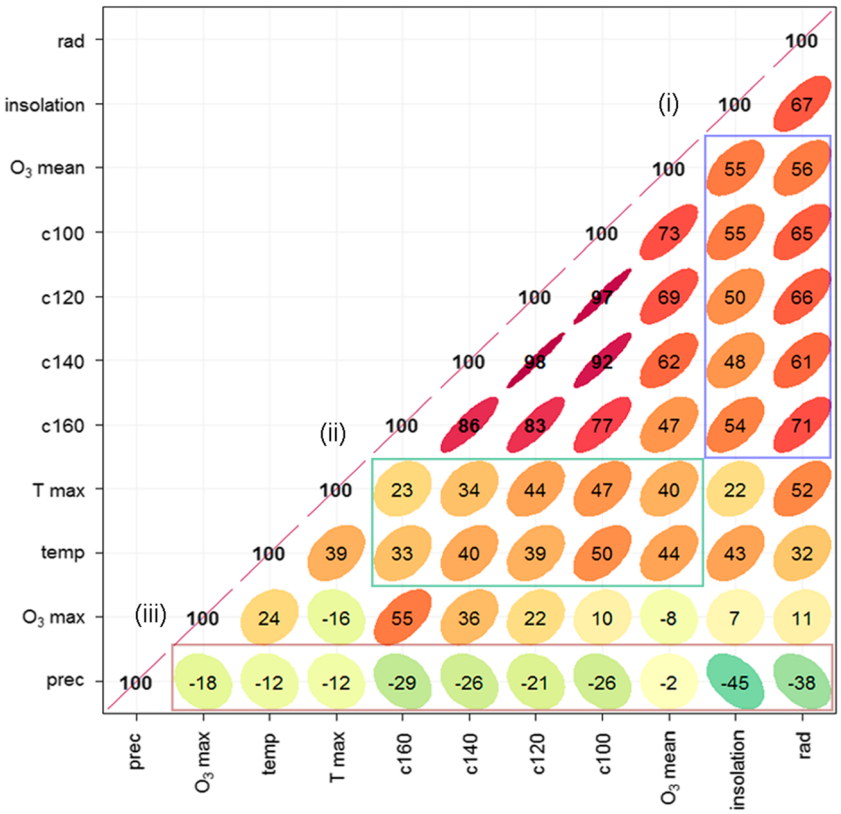

Fig. 14 Correlation of ozone (%) and meteorological variables (rad = radiation, insolation, T_{max} = daily maximum temperature, temperature and prec = precipitation), c160–c100 are the number of cases.

Figure 14 shows the ozone concentration at Ibirapuera site from 14 to 30 September. The black line is the observed ozone, and the color lines are the predicted by the LRM (in green) and by the QRM (in blue). Both models can represent the daily ozone pattern and the influence of the local variables.

Figure 15 shows the matrix of correlation between the ozone data (number of days per number of stations that exceeded 160, 140, 120, and 100 μg m^{-3} limit, mean and maximum ozone concentration) and meteorological variables (global solar radiation, hours of sunlight, rainfall, mean and maximum temperature).

Figure 15 shows the correlation of the global solar radiation and hours of sunlight, grouped (i) as the blue rectangle (Pope et al. 2002), and has the same order (and positive) of the correlation of the gasohol and diesel suggesting that both variables are equally important to explain the ozone trends. The mean and maximum temperature correlation, grouped with the green rectangle (ii), is relatively low. The precipitation

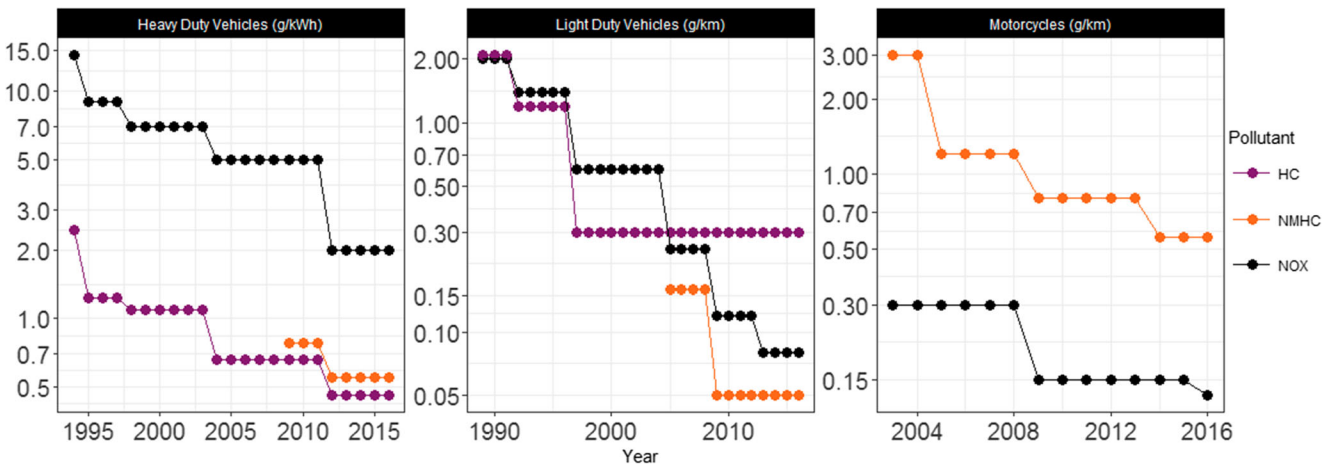

Fig. 15 Emissions standards for HDV (g kWh^{-1}), LDV (g km^{-1}) (4-stroke engines), and MC (g km^{-1})

influence is related with some features previously discuss in the introduction, such the relation of precipitation and nebulosity that can be visualized by the negative correlation with the number of cases and ozone concentrations along the correlation grouped on the red rectangle (iii).

Vehicular emissions

It has been shown that vehicles are the most important source of ozone precursors in São Paulo (Andrade et al. 2012; CETESB 2014). Hence, reviewing a description of this source and its controlling actions is of great interest. The type of fuel consumed by the fleet consists of gasoline blended with approximately 27% ethanol (gasohol) and ethanol and diesel blended with 10% of biodiesel. The biofuels come mostly from sugar cane crops. Vehicles that entered in circulation between 1990 and 2007 have engines that consume ethanol. However, in 2003 vehicles with flex engines became available in the marked, these engines are capable of running with gasohol, ethanol or any mixture in between (Giroldo et al. 2005). In this way, the demand for gasohol or ethanol on flex vehicles depends on the price. As consequence, in the last 15 years, the number of vehicles in circulation increased, being ethanol with 41.5%, gasohol with 52.4%, and diesel with 6.1%.

Regarding the vehicular emissions standards in Brazil, they follow the air pollution control program by motor vehicles (PROCONVE) and air pollution control program for motorcycles (PROMOT), which sets limits for vehicular emissions of light and heavy-duty vehicles, and motorcycles (IBAMA 2011). Figure 16 shows the exhaust emissions standards for HDV, PC, and MC for NOX and HC and NMHC for new vehicles. All the standards show a pattern of restricting the standards to newer models every few years. HDV are allowed to emit more NOX than HC. In the case of LDV, older vehicles have similar limits around 2 g km^{-1}; however, since 1997, the standards for HC was kept constant in 0.3 g km^{-1}, the NMHC limits started in 2005 with 0.16 g km^{-1} which dropped to 0.05 g km^{-1}, and the NOX limits changed till reach 0.08 g km^{-1}.

Figure 16 shows the matrix of correlation between the ozone data (number of days per number of stations that exceeded 160, 140, 120, and 100 μg m^{-3} limit, mean and maximum ozone concentration), and the fuel sales (gasohol, ethanol, diesel, and total fuel).

This figure shows a significant positive correlation between the number of cases (c160–c100) and the fuel sales of gasohol (gas), ethanol (eth) and diesel (die), as the total fuel sales, grouped on the blue rectangle (i), when the ozone limit decreases the correlation increases, on the other hand, the

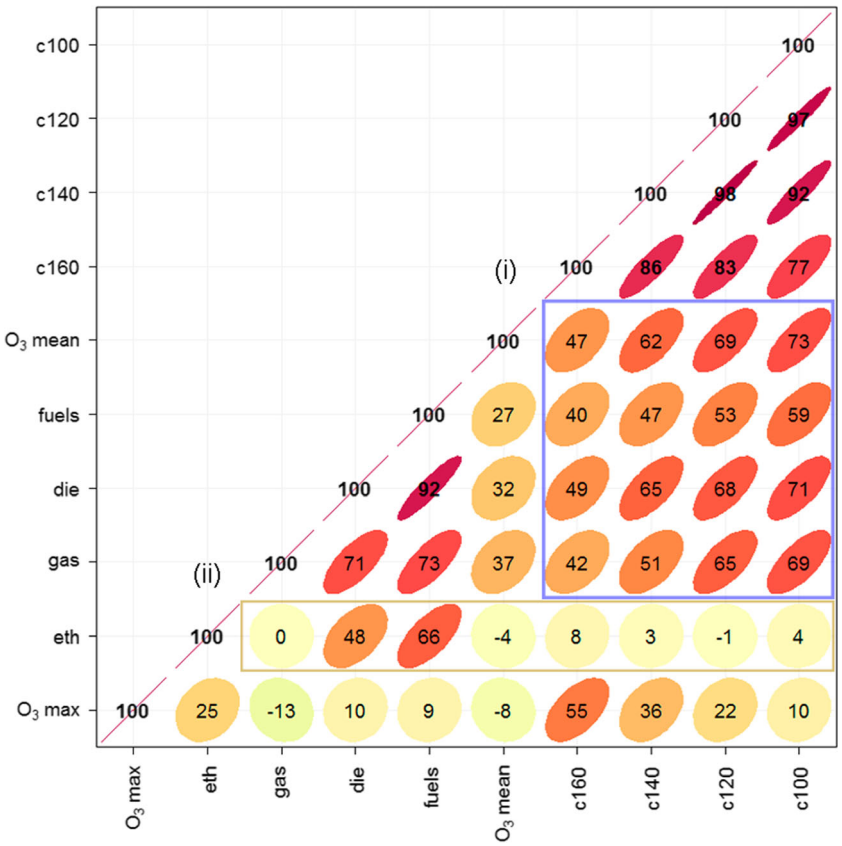

Fig. 16 Correlation of ozone data against fuel sales. eth = ethanol sales, gas = gasohol sales, die = diesel sales, c160–c100 are the number of cases

Table 2 Ozone tendency by season (μg m^{-3} $year^{-1}$)

Site	Spring	Summer	Autumn	Winter
Cubatão-Centro	– 0.80	– 0.28	– 0.97	*– 1.17**
Cubatão-Vale do Mogi	1.08	0.92	0.59	0.07
Diadema	– 0.61	0.48	– 1.05	– 0.44
Ibirapuera	0.02	0.30	– 0.69	*– 0.93**
Mauá	– 0.05	0.93	0.08	0.56
Moccá	*1.22**	*1.56**	0.70	0.30
Nossa S. do Ó	*1.16**	*2.05**	0.20	0.45
Santana	0.40	*1.88**	– 0.47	*– 1.10**
Santo André-Capuava	0.75	*2.46**	0.08	0.08
São Caetano do Sul	0.05	– 0.16	*– 1.01**	– 0.72
São José dos Campos-Jd. Satélite	– 1.01	0.30	– 0.84	*– 1.03**
Santo Amaro	– 1.14	– 1.00	*– 2.28**	– 1.36
Sorocaba	– 0.25	– 0.33	– 0.08	0.73
Parque Dom Pedro II	– 0.83	– 0.46	*– 1.74**	– 1.24
Paulinia	1.34	0.48	0.08	0.55
Pinheiros	– 0.63	– 0.97	*– 1.41**	*– 1.37**

*Significant values

ethanol sales (grouped on the yellow rectangle (ii)) does not explain the ozone annual variability.

The fuel consumption can give a general idea of the evolution of the vehicular emissions along the time and show some features of the vehicular activity. But the use of emission factors rather than emission standards can give a better estimative of the vehicular emissions.

Spatial variability

The time series of mean or maximum ozone does not give a picture of the spatial distribution or the changes in the spatial distribution over time at the São Paulo Macrometropolis. For this reason, the complete ozone time series was grouped in four seasons and analyzed individually by each site (Table 2). In Table 2, we present the tendency of ozone concentrations (μg m^{-3} $year^{-1}$) for each site by season. Trends with statistical significance (p value < 0.01) are set in italics.

The positive trends occur only in the warmer months of the spring and summer (months that preset typically high ozone concentrations) while the negative ones occur in the colder months. The strongest trends are Santo André-Capuava (which 2.46 μg m^{-3} by year), Nossa S. do Ó (2.05 μg m^{-3} by year) and Santana (1.88 μg m^{-3} by year) with positive (increase ozone concentrations) values and Santo Amaro (-2.28 μg m^{-3} by year), Parque Dom Pedro II (− 1.74 μg m^{-3} by year), and Pinheiros (− 1.41 μg m^{-3} by year) with negative (decreasing ozone concentrations) values. Figure 17 presents the images of spatial location for the MASP sites with their differences in terms of urban structure. Positive trends are indicated by red circles and the negatives by the blue ones. The absolute values (largest value for all seasons) are represented by the circle diameter for the significant trends.

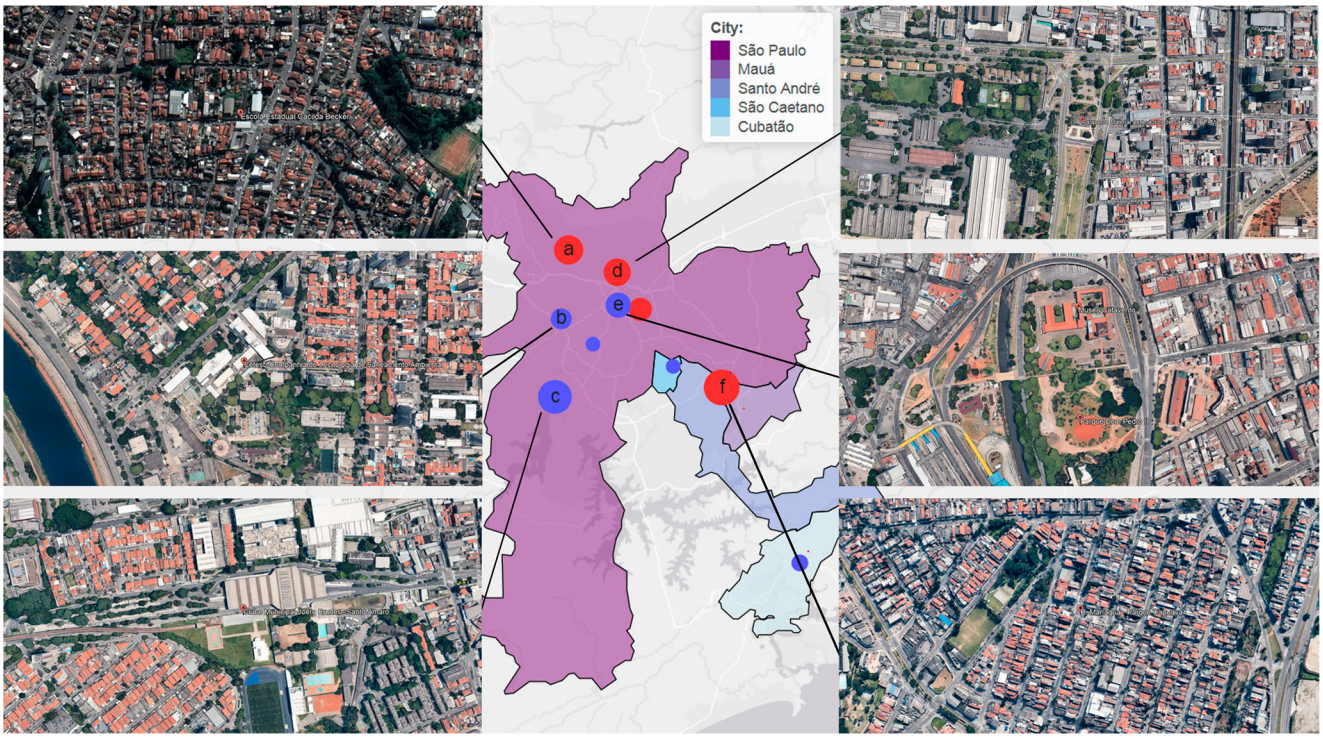

Fig. 17 Images of (a) Nossa S. do Ó, (b) Pinheiros, (c) Santo Amaro, (d) Santana, (e) Parque Dom Pedro II, and (f) Santo André-Capuava

The sites that present the strongest negative trends are those with the presence of trees or those in residential areas near the parks. On the other hand, positive trends occur in highly urbanized areas and near to highways, except Moocá station, which is in a residential region with a park in the neighborhood, that exhibit a strong positive trend.

Monitoring stations in the neighborhood of the main streets present with the negative trend for the ozone concentration (the opposite is observed for the distant stations). This behavior would be due to the reduction of NO_X and VOC emissions in these regions, which in general, contributes to the VOC/NO_X ratio resulting in a lower amount of ozone. For the stations relatively far away from the streets (with a lower direct contribution of vehicular emissions), the emissions from fixed sources (such as painting activities, factories, restaurants, and other sources) and the lower emissions of NO_X contribute to the positive trend of the ozone concentrations.

Conclusions

The concentrations of ozone measured at São Paulo Macrometropolis are summarized and compared with different standards that produce very distinct pictures of the air quality across 22 years of data. The use of 8-h moving averages in the time series of the ozone concentration masks the daily pattern, which is the main pattern observed for this variable, but can be useful for another comparisons, like population exposure and comparison with international standards.

The variability of ozone in different time scales is presented, and the ozone concentrations exhibit well-defined daily and seasonal patterns. The long-term trend of the mean ozone concentration, maximum ozone concentration, or the number of occurrences of ozone concentrations greater than 100, 120, 140, and 160 μg m^{-3} were investigated, but no clear temporal trend was found. Additional comparison with some climate indexes (ESRL 2018) such as SOI, AMO, PDO, and Madden-Julian (not shown) did not explain the variation of ozone in time scale of many years.

To explain the variability of ozone, we adopted a quantile regression model (QRM) using the hourly ozone concentration measured at Ibirapuera station as a dependent variable and the CO, NO, NO_2, wind speed, temperature, and incident solar radiation as explanatory (independent) variables, and 0.76% of the variability of the ozone can be explained by these local variables. The QRM analysis presented showed good agreement with observed ozone data and the QRM produces similar results (not shown) when applied for other stations (Cubatão-Centro, Pinheiros, São Caetano do Sul and Sorocaba) presenting the same patterns for wind speed, temperature, and radiation but small differences for NO, NO_2, and CO.

Some of the individual stations present significant trend of the ozone (both positive and negative trends) over the time series, the positive trends occur in sites in the proximity of busy roads, and the negative ones in residential areas next to trees. These local ozone trends are more likely to be related to changes in traffic and urbanization process that can change how the ozone precursors are released in the atmosphere. Although the results point to a decrease in the ozone concentration in the coldest season in some sites, this does not represent a gain in terms of air quality, since those months are months where this concentration is naturally lower, on the other hand the increase in concentration in the warmer season is an indication that the air quality it is getting worse in these locations and in their neighborhood.

The control of the air quality in metropolitan areas such as São Paulo Macrometropolis can be a challenge, not only because of the nonlinear response of ozone to the changes in emissions or the dependency of many other factors like the weather that are responsible for control the transport of pollutants, precursors and photochemistry, but also mainly because of the strong influence of the human activity in many aspects such as economics (technology, fuel used, and degradation of the vehicles in circulation), transport (intensity of use and traffic congestion), and politics (standards of emissions and limits of exposure).

Acknowledgements The authors would like to thank the São Paulo State Environmental Agency (CETESB) for the air quality data used in this work and to IAG Weather Station (www.estacao.iag.usp.br) for the meteorological data provided.

Funding information The authors would like to thank to the Coordenação de Aperfeiçoamento de Pessoal de Nível Superior (CAPES) and Fundação de Amparo à Pesquisa do Estado de São Paulo (FAPESP) for the financial support and the National Council for Scientific and Technological Development (Conselho Nacional de Desenvolvimento Científico e Tecnológico [CNPq]) processes /2018-0 and 306862/2018-2.

References

Ainsworth EA (2017) Understanding and improving global crop response to ozone pollution. Plant J **90**(5):886–897

ALESP (2013) Decreto n° 59.113 , de 23/04/2013. 2013.

Alvim DS, Gatti LV, Corrêa SM, Chiquetto JB, Santos GM, Rossatti CS, Pretto A, Rozante JR, Figueroa SN, Pendharkar J, Nobre P (2018) Determining VOCs Reactivity for Ozone Forming Potential in the Megacity of São Paulo. Aerosol Air Qual Res **18**:2460–2474

Anderson H, Atkinson R, Peacock J, Marston L, Konstantinou K (2004) Meta-analysis of time-series studies and panel studies of particulate matter (PM) and ozone (O3). Rep a WHO Task Gr. 1–68. Available from: *http://scholar.google.com/scholar?hl=en&btnG=Search&q=intitle: Meta-analysis+of+timeseries+studies+and+panel+studies+of+Particulate+Matter+(+PM+)+and+Ozone+(+O+3+)#0*

Andrade, M., Miranda, R. M., Fornaro, A., Kerr, A., Oyama, B., Andre, P. A., & Saldiva, P. (2012). Vehicle emissions and PM 2.5 mass concentrations in six Brazilian cities. Air Quality, Atmosphere & Health, **5**(1):79–88

Andrade MF, Kumar P, Freitas ED, Ynoue RY, Martins J, Martins LD, Nogueira T, Perez-Martinez P, de Miranda RM, Albuquerque T, Gonçalves FLT, Oyama B, Zhang Y (2017) Air quality in the

megacity of São Paulo: Evolution over the last 30 years and future perspectives. Atmos Environ **159**:66–82

Arjomandi M, Balmes JR, Frampton MW, Bromberg P, Rich DQ, Stark P, Alexis NE, Costantini M, Hollenbeck-Pringle D, Dagincourt N, Hazucha MJ (2018) Respiratory Responses to Ozone Exposure. MOSES (The Multicenter Ozone Study in Older Subjects). Am J Respir Crit Care Med **197**(10):1319–1327

Balajee Karthik L, Babu Sujith, Suliankatchi Rizwan A, Meena Sehgal, (2017) Characteristics of the Ozone Pollution and its Health Effects in India. International Journal of Medicine and Public Health **7**(1): 56–60

Baur D, Saisana M, Schulze N (2004) Modelling the effects of meteorological variables on ozone concentration—a quantile regression approach. Atmos Environ **38**:4689–4699

Bluestein HB (1992) Synoptic-dynamic meteorology in midlatitudes: Volume 1, principles of kinematics and dynamics

Brito J, Wurm F, Yáñez-Serrano AM, de Assunção JV, Godoy JM, Artaxo P (2015) Vehicular Emission Ratios of VOCs in a Megacity Impacted by Extensive Ethanol Use: Results of Ambient Measurements in São Paulo, Brazil. Environ Sci Technol **49**:11381–11387

Capotondi A, Wittenberg AT, Newman M, Di Lorenzo E, Yu J, Braconnot P, Cole J, Dewitte B, Giese B, Guilyardi E, Jin F, Karnauskas K, Kirtman B, Lee T, Schneider N, Xue Y, Yeh S (2015) Understanding ENSO Diversity. Bull Am Meteorol Soc **96**:921–938

Carter, W. P. (1994). Development of ozone reactivity scales for volatile organic compounds. Air & waste, **44**(7):881–899

Carvalho VSB, Freitas ED, Martins LD, Martins JA, Mazzoli CR, Andrade MF (2015) Air quality status and trends over the Metropolitan Area of São Paulo, Brazil as a result of emission control policies. Environ Sci Pol **47**:68–79

CETESB (2014) Qualidade do ar no estado de São Paulo, 2013. In *Série Relatórios* 110

CETESB (2018) QUALAR - Automatic air-quality monitoring stations network. CETESB

Conover WJ (1980) Practical Nonparametric Statistics

CONSELHO NACIONAL DO MEIO AMBIENTE (2018) Resolução CONAMA Nº 491/2018

CONSELHO NACIONAL DO MEIO AMBIENTE (1990) Resolução CONAMA Nº 003/90

Di Q, Dai L, Wang Y, Zanobetti A, Choirat C, Schwartz JD, Dominici F (2017) Association of short-term exposure to air pollution with mortality in older adults. Jama **318**(24):2446–2456

Dominutti PA, Nogueira T, Borbon A, Andrade MdF, Fornaro A (2016) Atmos Environ 142:371–382

EPA (1996) United States Environmental Agency (US-EPA): Code of Federal Regulation, Ambiente Air Surveillance. Ed. 1996

ESRL (2018) Climate Indices: Monthly Atmospheric and Ocean Time Series

Felzer BS, Cronin T, Reilly JM, Melillo JM, Wang X (2007) Impacts of ozone on trees and crops. Compt Rendus Geosci **339**(11-12):784–798

Freitas ED, Rozoff CM, Cotton WR, Dias PLS (2007) Interactions of an urban heat island and sea-breeze circulations during winter over the metropolitan area of São Paulo, Brazil. Bound-Layer Meteorol **122**: 43–65

Fujita EM, Campbell DE, Zielinska B, Sagebiel JC, Bowen JL, Goliff WS, Stockwell WR, Lawson DR (2003) Diurnal and weekday variations in the source contributions of ozone precursors in California's South Coast Air Basin. J Air Waste Manage Assoc 53(7):844–863

Gaffney JS, Marley NA (2009) The impacts of combustion emissions on air quality and climate – From coal to biofuels and beyond. Atmos Environ **43**:23–36

Giroldo MB, Werninghaus E, Coelho E, Makant W (2005) Development of 1.6 L flex fuel engine for Brazilian market. SAE International

Goodman JE, Zu K, Loftus CT, Lynch HN, Prueitt RL, Mohar I, Shubin SP, Sax SN (2018) Short-term ozone exposure and asthma severity: Weight-of-evidence analysis. Environ Res **160**:391–397

Grivas G, Dimakopoulou K, Samoli E, Papakosta D, Karakatsani A, Katsouyanni K, Chaloulakou A (2017) Ozone exposure assessment for children in Greece - Results from the RESPOZE study. Sci Total Environ **581-582**:518–529

Helsel DR, Hirsch RM (2002) Statistical Methods in Water Resources. Techniques of Water Resources Investigations, Book 4, Chapter A3., US Geological Survey

Holton JR (2004) An Introduction to Dynamic Meteorology, Academic Press

Hwang B, Chen Y, Lin Y, Wu X, Leo Lee Y (2015) Relationship between exposure to fine particulates and ozone and reduced lung function in children. Environ Res **137**:382–390

IAG (2018) Weather Station's Bulletin

IBAMA (2011) Manual PROCONVE/PROMOT

IBGE (2018) Instituto Brasileiro de Geografia e Estatística. Diretoria de Pesquisas. Coordenação de População e Indicadores Sociais. Estimativas da população residente para os municípios e para as unidades da federação com data de referência em 1º de julho de. https://biblioteca.ibge.gov.br/visualizacao/livros/liv101609.pdf Accessed 2 Dec 2018

Ibarra-Espinosa S, Ynoue R, O'Sullivan S, Pebesma E, Andrade MDF, Osses M (2018) VEIN v0.2.2: an R package for bottom–up vehicular emissions inventories. Geosci Model Dev **11**:2209–2229

Jacobson MZ (2005) Fundamentals of Atmospheric Modeling, Cambridge University Press, USA

Koenker R, d'Orey V (1987) Computing regression quantiles. Appl Stat **36**:383–393

Koenker R, Machado JAF (1999) Goodness of Fit and Related Inference Processes for Quantile Regression. J Am Stat Assoc 94:1296–1310

Krzyzanowski M, Cohen A (2008) Update of WHO air quality guidelines. Air Quality, Atmosphere & Health **1**(1):7–13

Künzli N, Kaiser R, Medina S, Studnicka M, Chanel O, Filliger P, Herry M, Horak F, Puybonnieux-Texier V, Quénel P, Schneider J, Seethaler R, Vergnaud JC, Sommer H (2000) Public-health impact of outdoor and traffic-related air pollution: a European assessment. Lancet **356**:795–801

Landrigan PJ, Fuller R, Acosta NJR, Adeyi O, Arnold R, Basu N, Baldé AB, Bertollini R, Bose-O'Reilly S, Boufford JI, Breysse PN, Chiles T, Mahidol C, Coll-Seck AM, Cropper ML, Fobil J, Fuster V, Greenstone M, Haines A, Hanrahan D, Hunter D, Khare M, Krupnick A, Lanphear B, Lohani B, Martin K, Mathiasen KV, McTeer MA, Murray CJL, Ndahimananjara JD, Perera F, Potočnik J, Preker AS, Ramesh J, Rockström J, Salinas C, Samson LD, Sandilya K, Sly PD, Smith KR, Steiner A, Stewart RB, Suk WA, van Schayck OCP, Yadama GN, Yumkella K, Zhong M (2018) The Lancet Commission on pollution and health. Lancet **391**:462–512

Leila Droprinchinski Martins, Caroline Fernanda Hei Wikuats, Mauricio Nonato Capucim, Daniela S. de Almeida, Silvano Cesar da Costa, Taciana Albuquerque, Vanessa Silveira Barreto Carvalho, Edmilson Dias de Freitas, Maria de Fátima Andrade, Jorge Alberto Martins, (2017) Extreme value analysis of air pollution data and their comparison between two large urban regions of South America. Weather and Climate Extremes **18**:44–54

Leiva MA, Santibañez DA, Ibarra S, Matus P, Seguel R (2013) A five-year study of particulate matter (PM2.5) and cerebrovascular diseases. Environ Pollut **181**:1–6

Levy JI, Chemerynski SM, Sarnat JA (2005) Ozone Exposure and Mortality. Epidemiology **16**:458–468

Mantua NJ, Hare SR, Zhang Y, Wallace JM, Francis RC (1997) A Pacific Interdecadal Climate Oscillation with Impacts on Salmon Production. Bull Am Meteorol Soc **78**:1069–1079

Martins LD, Andrade MdF, Ynoue RY, Albuquerque ÉL d, Tomaz E, Vasconcellos P d C (2008) Ambiental volatile organic compounds in the megacity of São Paulo. Química Nova **31**(8):2009–2013

Monn C (2001) Exposure assessment of air pollutants: a review on spatial heterogeneity and indoor/outdoor/personal exposure to suspended particulate matter, nitrogen dioxide and ozone. Atmos Environ **35**: 1–32

Nair KN, Freitas ED, Sanchez-Ccoyllo OR, Dias M, Dias PLS, Andrade MF, Massambani O (2004) Dynamics of urban boundary layer over São Paulo associated with mesoscale processes. Meteorog Atmos Phys **86**:87–98

Nogueira T, Dominutti PA, de Carvalho LRF, Fornaro A, & de Fatima Andrade M (2014) Formaldehyde and acetaldehyde measurements in urban atmosphere impacted by the use of ethanol biofuel: Metropolitan Area of Sao Paulo (MASP), Fuel **134**:505–513

Nogueira T, Souza KF d, Fornaro A, Andrade M d F, Carvalho LRF d (2015) On-road emissions of carbonyls from vehicles powered by biofuel blends in traffic tunnels in the Metropolitan Area of Sao Paulo, Brazil. Atmos Environ **108**:88–97

Orlando JP, Alvim DS, Yamazaki A, Corrêa SM, Gatti LV (2010) Ozone precursors for the São Paulo metropolitan area. Sci Total Environ 408(7):1612–1620

Pérez-Martínez PJ, Andrade MF, Miranda RM (2015) Traffic-related air quality trends in São Paulo, Brazil. J Geophys Res-Atmos **120**: 6290–6304

Pope IC, Burnett RT, Thun MJ et al (2002) Lung Cancer, Cardiopulmonary Mortality, and Long-term Exposure to Fine Particulate Air Pollution. JAMA **287**:1132–1141

Qin Y, Tonnesen GS, Wang Z (2004) Weekend/weekday differences of ozone, NOx, Co, VOCs, PM10 and the light scatter during ozone season in southern California. Atmos Environ **38**:3069–3087

Reimann C, Filzmoser P, Garrett R Dutter R (2008) Statistical Data Analysis Explained: Applied Environmental Statistics with R, John Wiley & Sons, Ltd.

Rosiberto Salustiano da Silva Júnior, Marcio Gledson Lopes de Oliveira, Maria de Fátima Andrade, (2009) Weekend/weekday differences in concentrations of ozone, nox, and non-methane hydrocarbon in the metropolitan area of São Paulo. Revista Brasileira de Meteorologia **24**(1):100–110

Stull RB (1988) An introduction to boundary layer meteorology. Kluwer Academic Publishers, Dordrecht

Theil H (1992) A rank-invariant method of linear and polynomial regression analysis. In: Raj B, Koerts J (eds) Henri Theil's Contributions to Economics and Econometrics: Econometric Theory and Methodology. Springer Netherlands, Dordrecht, pp 345–381

van Zelm R, Huijbregts MAJ, den Hollander HA, van Jaarsveld HA, Sauter FJ, Struijs J, van Wijnen HJ, van de Meent D (2008) European characterization factors for human health damage of PM10 and ozone in life cycle impact assessment. Atmos Environ **42**:441–453

Weschler CJ (2006) Ozone's Impact on Public Health: Contributions from Indoor Exposures to Ozone and Products of Ozone-Initiated Chemistry. Environ Health Perspect **114**:1489–1496

WHO (2000) Air quality guidelines for Europe. In WHO Regional Publications, European Series, No. 91

WHO (2016) Ambient air pollution: a global assessment of exposure and burden of disease